1521-0111/12/8202-199–208$25.00
MOLECULAR PHARMACOLOGY
Vol. 82, No. 2
76687/3781600

Mol Pharmacol 82:199–208, 2012

The Synaptic Vesicle Glycoprotein 2A Ligand Levetiracetam Inhibits Presynaptic Ca^{2+} Channels through an Intracellular Pathway[S]

Christian Vogl, Sumiko Mochida, Christian Wolff, Benjamin J. Whalley, and Gary J. Stephens

School of Pharmacy, University of Reading, Reading, United Kingdom (C.V., B.J.W., G.J.S.); Department of Physiology, Tokyo Medical University, Tokyo, Japan (S.M.); and UCB Centre for CNS Innovation, UCB Pharma, CNS Research, Braine-l'Alleud, Belgium (C.W.)

Received November 4, 2011; accepted May 3, 2012

ABSTRACT

Levetiracetam (LEV) is a prominent antiepileptic drug that binds to neuronal synaptic vesicle glycoprotein 2A protein and has reported effects on ion channels, but with a poorly defined mechanism of action. We investigated inhibition of voltage-dependent Ca^{2+} (Ca_V) channels as a potential mechanism through which LEV exerts effects on neuronal activity. We used electrophysiological methods to investigate the effects of LEV on cholinergic synaptic transmission and Ca_V channel activity in superior cervical ganglion neurons (SCGNs). In parallel, we investigated the effects of the inactive LEV *R*-enantiomer, (*R*)-α-ethyl-2-oxo-1-pyrrolidine acetamide (UCB L060). LEV but not UCB L060 (each at 100 μM) inhibited synaptic transmission between SCGNs in long-term culture in a time-dependent manner, significantly reducing excitatory postsynaptic potentials after a ≥30-min application. In isolated SCGNs, LEV pretreatment (≥1 h) but not short-term application (5 min) significantly inhibited whole-cell Ba^{2+} current (I_{Ba}) amplitude. In current-clamp recordings, LEV reduced the amplitude of the afterhyperpolarizing potential in a Ca^{2+}-dependent manner but also increased the action potential latency in a Ca^{2+}-independent manner, which suggests additional mechanisms associated with reduced excitability. Intracellular LEV application (4–5 min) caused rapid inhibition of I_{Ba} amplitude, to an extent comparable to that seen with extracellular LEV pretreatment (≥1 h). Neither pretreatment nor intracellular application of UCB L060 produced any inhibitory effects on I_{Ba} amplitude. These results identify a stereospecific intracellular pathway through which LEV inhibits presynaptic Ca_V channels; resultant reductions in neuronal excitability are proposed to contribute to the anticonvulsant effects of LEV.

Introduction

LEV is a third-generation AED that is prescribed as monotherapy for the treatment of partial-onset seizures, with or without secondary generalization, and as adjunctive therapy for the treatment of partial-onset seizures, myoclonic seizures, and primary, generalized, tonic-clonic seizures (Schiemann-Delgado et al., 2012). Compared with many other currently available AEDs, LEV has an exceptionally high safety margin and favorable side effect profile (Klitgaard et al., 1998), with unique pharmacokinetic properties and broad-spectrum anticonvulsant effects (Grünewald, 2005; De Smedt et al., 2007a,b). The anticonvulsant profile of LEV was proposed to be mediated through binding to a novel molecular target, SV2A (Lynch et al., 2004), for which more-potent and functionally diverse ligands, including brivaracetam, have been developed (Kenda et al., 2004; Matagne et al., 2008; Gillard et al., 2011). SV2A is ubiquitously expressed in presynaptic terminals (Bajjalieh et al., 1992, 1994; Feany et al., 1992) and is essential for Ca^{2+}-dependent vesicular neurotransmitter release (Xu and Bajjalieh, 2001; Custer et al., 2006; Chang and Südhof, 2009). Therefore, the anticonvulsant actions of LEV may involve modification of SV2A-mediated, dysregulated, neurotransmitter release. LEV reduced kindling-induced SV2A increases (Matveeva et al., 2008) and demonstrated decreased anticonvulsant efficacy in vivo in

This work was supported by a UCB Pharma investigator-initiated nonclinical study studentship award and a Japan Society for the Promotion of Science short-term fellowship.

B.J.W. and G.J.S. contributed equally to this work.

Article, publication date, and citation information can be found at http://molpharm.aspetjournals.org.
http://dx.doi.org/10.1124/mol.111.076687.

[S] The online version of this article (available at http://molpharm.aspetjournals.org) contains supplemental material.

ABBREVIATIONS: LEV, levetiracetam; AP, action potential; AED, antiepileptic drug; AHP, afterhyperpolarizing potential; Ca_V, voltage-dependent Ca^{2+}; EPSP, excitatory postsynaptic potential; ECS, extracellular solution; I_{Ba}, Ba^{2+} current; K_V, voltage-dependent K^+; PBS, phosphate-buffered saline; PPP, phase plane projection; SCG, superior cervical ganglion; SCGN, superior cervical ganglion neuron; SV2A, synaptic vesicle glycoprotein 2A; UCB L060, (*R*)-α-ethyl-2-oxo-1-pyrrolidine acetamide.

heterozygous SV2A mice (Kaminski et al., 2009). LEV could reverse deficits in synaptic transmission induced by SV2A overexpression (Nowack et al., 2011). It was proposed that LEV action might be mediated by vesicular entry through SV2A binding (Meehan et al., 2011); however, downstream mechanisms through which SV2A ligands reduce neuronal excitability remain to be elucidated.

LEV inhibited excitatory transmission in hippocampal CA1 neurons (Yang et al., 2007; Yang and Rothman, 2009; Meehan et al., 2011) and dentate gyrus cells (Lee et al., 2009) and was reported to modulate neuronal excitability through effects on voltage-dependent ion channels (Surges et al., 2008). Although LEV did not affect Na^+- and low-voltage-activated Ca_V channels (Zona et al., 2001), it was reported to inhibit high-voltage-activated Ca_V channels; those effects occurred in response to short-term LEV application (Lukyanetz et al., 2002; Pisani et al., 2004; Costa et al., 2006; Martella et al., 2008), although one study reported that LEV action on Ca_V channels required prolonged exposure (Niespodziany et al., 2001). LEV inhibition of delayed rectifier K^+ channels also was reported (Madeja et al., 2003). Moreover, brivaracetam and seletracetam inhibit Na^+ channels and high-voltage-activated Ca_V channels, respectively (Martella et al., 2009; Zona et al., 2010), which suggests distinct, direct, ion channel blockade by different SV2A ligands, although it remains unclear whether effects on ion channels are independent of SV2A-mediated interactions.

Here, we use superior cervical ganglion neurons (SCGNs) as a useful system to investigate LEV modulation of synaptic transmission and presynaptic Ca_V channels (Mochida et al., 2003; Stephens and Mochida, 2005; Bucci et al., 2011). Overall, short-term extracellular LEV effects were not seen, and our data support LEV acting through an intracellular pathway to inhibit Ca_V channels, consistent with a longer-term reduction in synaptic transmission that might underlie LEV's mechanism of action as an AED.

Materials and Methods

Tissue Culture Methods

SCGNs for Patch-Clamp Recordings. Neurons were dissociated from freshly isolated superior cervical ganglia (SCGs) of 3- to 6-week-old, male, Wistar rats, as described previously (Bucci et al., 2011). Rats were euthanized with a schedule 1 method, in accordance with UK Home Office regulations [Animals (Scientific Procedures) Act 1986]. Immediately after dissection, SCGs were desheathed, cut into small fragments with fine irridectomy scissors in L-15 medium (Sigma-Aldrich, Poole, Dorset, UK) supplemented with 5% penicillin/streptomycin (Invitrogen, Carlsbad, CA), and transferred to a tube containing modified L-15 enzyme solution (0.5 mg/ml trypsin, 1 mg/ml collagenase, and 3.6 mg/ml glucose; all from Sigma-Aldrich), for 30 min at 37°C. Enzymatic reactions were blocked with the addition of growth medium containing 84% Eagle's minimal essential medium, 10% fetal calf serum, 5% horse serum (all from Lonza Wokingham Ltd., Wokingham, Berkshire, UK), and 1% penicillin/streptomycin (Invitrogen). The resulting cell suspension was centrifuged at 1000 rpm for 6 min, and the pellet was resuspended in growth medium. Cells were plated onto glass coverslips coated with poly-L-ornithine (0.5 mg/ml; Sigma-Aldrich) and were incubated overnight in a water-saturated incubator (37°C, with 5% CO_2).

Long-Term SCGN Cultures for Microelectrode Recordings. Neurons were dissociated and cultured as described previously (Mochida et al., 1995). Wistar rats (postnatal day 7) were anesthetized with diethyl ether and decapitated, according to the guidelines of the Physiological Society of Japan. SCGs were desheathed, incubated in L-15 medium (Invitrogen) containing 0.5 mg/ml collagenase (Worthington Biochemicals, Freehold, NJ), and gently triturated. After washing, centrifugation (1300 rpm, 3 min), and resuspension, isolated neurons were plated and maintained in a water-saturated incubator (37°C, with 5% CO_2) for 5 to 6 weeks, in growth medium composed of 84% Eagle's minimal essential medium, 10% fetal calf serum, 5% horse serum, 1% penicillin/streptomycin (all from Invitrogen), and 25 ng/ml nerve growth factor (2.5 S, grade II; Alomone Labs, Jerusalem, Israel). The medium was changed twice per week.

Electrophysiological Studies

Whole-Cell Voltage-Clamp Recordings. Coverslips containing SCGNs (24–36 h in short-term culture) were mounted in a recording chamber on an Olympus IX 51 microscope (Olympus, Tokyo, Japan) with differential interference contrast phase-contrast optics. Borosilicate glass capillaries (Harvard Apparatus Inc., Holliston, MA) were used to fabricate patch electrodes, which had resistances of 5 to 7 MΩ when filled with an intracellular solution consisting of 140 mM CsCl, 1 mM EGTA, 1 mM $MgCl_2$, 0.1 mM $CaCl_2$, 4 mM MgATP, and 10 mM HEPES (pH adjusted to 7.3 with CsOH). For isolation of Ca^{2+} currents, the extracellular solution contained 160 mM TEA bromide, 3 mM KCl, 1 mM $NaHCO_3$, 1 mM $MgCl_2$, 10 mM HEPES, 4 mM D-glucose, and 10 mM $BaCl_2$ (pH adjusted to 7.4 with Sigma-Aldrich 7–9 base). All recordings were performed at room temperature (20–22°C). Voltage-clamp data were acquired with an Axoclamp 200B patch-clamp amplifier (Molecular Devices, Sunnyvale, CA), digitized with a Digidata 1200 analog-digital converter (Molecular Devices), and analyzed with WinWCP 4.0.7 software (John Dempster, University of Strathclyde, Glasgow, UK). Capacitive transients and leak conductances were subtracted online by using a *P*/4 protocol. Current-voltage relationships were evoked with cumulative 10-mV depolarizing steps from a holding potential of −70 mV. For detection of drug effects, neurons were repetitively depolarized to a potential that produced peak I_{Ba} (typically from a holding potential of −70 mV to +10 mV for 50 ms at 0.1 Hz). Currents were normalized to cell capacitance (current density), and such relationships were fitted by applying a modified Boltzmann function of the form current = $G_{max}(V - V_{rev})/(1 + \exp[-(V - V_{0.5})/k])$, where G_{max} is the maximal conductance, $V_{0.5}$ is the half-activation potential (i.e., the voltage at which 50% of current is activated), V_{rev} is the null potential, and k is the slope factor (Stephens et al., 2000). Conductance-voltage relationships ($I/[V_m - E_{Ba}]$) were fitted with a standard Boltzmann function. Offline analysis was performed with WinWCP 4.0.7, Microsoft Office 2007 (Microsoft, Redmond, WA), OriginPro 7.0 (OriginLab Corp., Northampton, MA), and Minitab 16 (Minitab Inc., State College, PA) software. All data are presented as mean ± S.E.M. Statistical significance was determined by using nonparametric Mann-Whitney *U* tests for normalized data.

Whole-Cell Current-Clamp Recordings. Current-clamp recordings were performed with SCGNs (24–36 h in short-term culture) with borosilicate glass microelectrodes filled with an intracellular solution containing 150 mM KCl, 1 mM $CaCl_2$, 10 mM HEPES, 1 mM $MgCl_2$, 4 mM MgATP, 0.3 mM NaGTP, and 0.5 mM EGTA (pH adjusted to 7.3 with Sigma 7–9), with resistances of 5 to 7 MΩ. Cells were superfused with standard extracellular solution (ECS) consisting of 140 mM NaCl, 5 mM KCl, 2 mM $MgCl_2$, 10 mM HEPES, 2 mM $CaCl_2$, and 10 mM D-glucose (pH adjusted to 7.4 with Sigma 7–9) or with low-Ca^{2+} ECS containing 0.2 mM Ca^{2+} and 1.8 mM $MgCl_2$ in place of 2 mM Ca^{2+}. All data were acquired with an EPC-7 patch-clamp amplifier (HEKA, Lambrecht/Pfalz, Germany) digitized with a Digidata 1200 digitizer (Molecular Devices), and analyzed with WinWCP 4.0.7 software (John Dempster, University of Strathclyde). Resting membrane potentials were measured at currents of 0 pA. Intrinsic membrane properties of the recorded cells were determined with depolarizing current ramp injections from 0 to 500 pA over 1 s (0.5 pA/ms), and the first AP of the evoked train was used for detailed analysis; voltage data traces were preprocessed with low-pass filter-

ing, upscaling, and smoothing (first-order Butterworth filter, piecewise cubic hermite interpolating polynomial upscaling, and smoothing spline). Voltage phase plane projections (PPPs) were created by plotting voltage rate against membrane voltage, with thresholds defined as the value at which the AP rate of rise exceeded 3 times the S.D. of the respective baseline value (MATLAB; The MathWorks Inc., Natick, MA). Values for individual voltage rates for the depolarization and repolarization slopes were determined from the same PPPs measured at membrane voltages of 0 mV. Analyses were performed offline with WinWCP 4.0.7, OriginPro 7.0 (OriginLab Corp), and Minitab 16 (Minitab Inc.) software. Data are presented as mean ± S.E.M., and statistical significance was determined by using unpaired Student's *t* tests.

Synaptic Transmission between Long-Term Cultured SCGNs. Paired intracellular recordings were performed with proximal neurons that had been cultured for 5 to 6 weeks, as described previously (Mochida et al., 1995). In brief, neurons were observed with a Nikon Diaphot 300 microscope (Nikon, Tokyo, Japan) equipped with differential interference contrast phase-contrast optics. Microelectrodes were filled with an intracellular solution composed of 1 M potassium acetate, 3.3 mM MgATP, and 6.7 mM NaHEPES and had resistances of 70 to 100 MΩ. SCGNs were superfused with an extracellular solution containing 136 mM NaCl, 5.9 mM KCl, 2.5 mM $CaCl_2$, 1.2 mM $MgCl_2$, 11 mM glucose, and 3 mM NaHEPES (pH adjusted to 7.4 with NaOH). Data were acquired with Nihon Kohden MEZ-8201 microelectrode amplifiers (Nihon Kohden, Tokyo, Japan), digitized with a Digidata 1440 digitizer (Molecular Devices), and analyzed with pClamp 10 software (Molecular Devices). Presynaptic AP generation was triggered at 0.1 Hz with a Nihon Kohden SEN-3301 electronic stimulator, and EPSPs were recorded from the partner cell. Analyses were conducted offline with pClamp 10 (Molecular Devices), OriginPro 7.0 (OriginLab Corp.), and Minitab 16 (Minitab Inc.) software. Data are presented as either normalized mean ± S.E.M. values or mean values smoothed with an eight-point, moving-average algorithm. Statistical significance was determined by using Mann-Whitney *U* tests for normalized data.

Protein Expression and Fluorescence Microscopy

Western Blot Analysis of Protein Expression. Protein samples were obtained from tissue samples (SCG, cortex, heart, and liver) from five male Wistar rats (at least 3 weeks of age) per experiment and were homogenized (Precellys 24; VWR, Leuven, Belgium) in CellyticM lysis buffer (Sigma-Aldrich) supplemented with a serine/cysteine protease inhibitor mixture (Complete Mini EDTA-free; Roche Diagnostics, Burgess Hill, UK). Samples were subsequently separated through SDS-polyacrylamide gel electrophoresis, transferred to nitrocellulose membranes (GE Healthcare, Chalfont St. Giles, Buckinghamshire, UK), and probed with specific polyclonal rabbit anti-SV2A antibody (1:1000; Synaptic Systems, Göttingen, Germany). Antibody binding was detected by using secondary antibodies conjugated with horseradish peroxidase (1:5000; Sigma-Aldrich), which reacted with enhanced chemiluminescence solution (GE Healthcare), and samples were observed on an imaging platform (Syngene Europe, Cambridge, UK).

Immunocytochemical Analyses and Epifluorescence Microscopy. SCGNs in short-term culture were fixed in Dulbecco's PBS supplemented with 4% (v/v) paraformaldehyde and 4% (w/v) sucrose (VWR) and then were permeabilized with PBS containing 0.25% Triton X-100. After 30 min of blocking in PBS with 0.05% Triton X-100, 1% (w/v) bovine serum albumin, and 2% (v/v) fetal bovine serum, cells were probed with primary antibodies against SV2A and synaptotagmin-1 (both at 1:200; Synaptic Systems). All primary antibodies were diluted in blocking buffer and applied for 1 h at room temperature, and then cells were fluorescently labeled for 1 h with Alexa Fluor 488-conjugated secondary antibodies (1:1000; Invitrogen). Specimens were observed with an AxioImager microscope equipped with Axiovision software (Carl Zeiss Ltd., Welwyn Garden City, UK). Images were obtained with a cooled, low-noise, charge-coupled device camera (Carl Zeiss Ltd.) and customized filters in blue (4′,6-diamidino-2-phenylindole) and green (Alexa Fluor 488/SV2A) channels, for all described conditions.

Pharmacological Assays. LEV (the *S*-enantiomer of α-ethyl-2-oxo-1-pyrrolidine acetamide) (Klitgaard et al., 1998) and its *R*-enantiomer, (*R*)-α-ethyl-2-oxo-1-pyrrolidine acetamide (UCB L060), were kind gifts from UCB Pharma SA (Brussels, Belgium). For short-term bath application, compounds were diluted in the respective extracellular solutions. For pretreatment, all compounds [LEV, UCB L060, and vehicle (reverse osmosis-purified water)] were diluted in growth medium and applied at the indicated times before the experiment. LEV and UCB L060 were used at final concentrations of 100 μM throughout; LEV has a pIC_{50} of 5.9 for its binding site in rat brain (Gillard et al., 2011), and the 100 μM concentration used should ensure >95% receptor occupancy. Clinically effective in vivo doses of LEV (1–3 g daily) yield peak plasma levels of 90 to 250 μM (Patsalos, 2000).

Results

SCGNs Express SV2A Protein. SV2A represents the binding protein for LEV (Lynch et al., 2004); therefore, we first established the expression of SV2A in SCGNs. A specific polyclonal anti-SV2A antibody showed strong labeling in isolated SCGNs but not supporting cells, which indicates neuron-specific SV2A expression (Supplemental Fig. 1). For further assessment of SV2A protein expression, samples from SCG tissue explants, cortex (positive control samples, tested at 10 and 20 μg of protein per sample), and heart and liver (negative control samples, tested at 20 μg of protein per sample) were probed with anti-SV2A antibody through Western blotting (Supplemental Fig. 1). The antibody recognized a ~90-kDa protein (the predicted molecular mass for SV2A) in all samples from neuronal tissues but not in samples from heart or liver. These results establish that isolated SCGNs express the LEV binding protein SV2A.

LEV Inhibits Synaptic Transmission in SCGNs. We next investigated the effects of the archetypical SV2A ligand LEV on synaptic transmission in long-term SCGN cultures, an appropriate model for studying fast cholinergic neurotransmission and modulation of presynaptic Ca_V channels (Mochida et al., 2003; Stephens and Mochida, 2005; Bucci et al., 2011). Extracellular application of LEV (100 μM) significantly reduced EPSP amplitudes recorded in synaptically coupled cells (Fig. 1, A, C, and D). Application of the LEV *R*-enantiomer, UCB L060, which has a reported SV2A binding affinity 1000-fold lower than that of LEV (Gillard et al., 2003, 2006) and so acted as a stereospecific control throughout the present study, did not affect EPSP amplitude (Fig. 1, B, C, and D). The inhibitory action of LEV showed a clear time dependence; ≥30 min was required for significant reductions in synaptic transmission, in comparison with UCB L060, and maximal effects were observed at 50 min (Fig. 1D). Thus, LEV, but not UCB L060, caused time-dependent inhibition of evoked transmitter release in SCGN synapses.

LEV Pretreatment, but Not Short-Term Application, Blocks Whole-Cell Ca^{2+} Current in SCGNs. Reductions in cholinergic transmission in SCGN synapses have been associated with inhibition of presynaptic Ca_V channels (predominantly $Ca_V2.2$-mediated N-type current) (Mochida et al., 1995, 2003), and LEV was reported to modulate neuronal $Ca_V2.2$ N-type current (Surges et al., 2008). Therefore, we investigated the effects of LEV on whole-cell Ca^{2+} currents

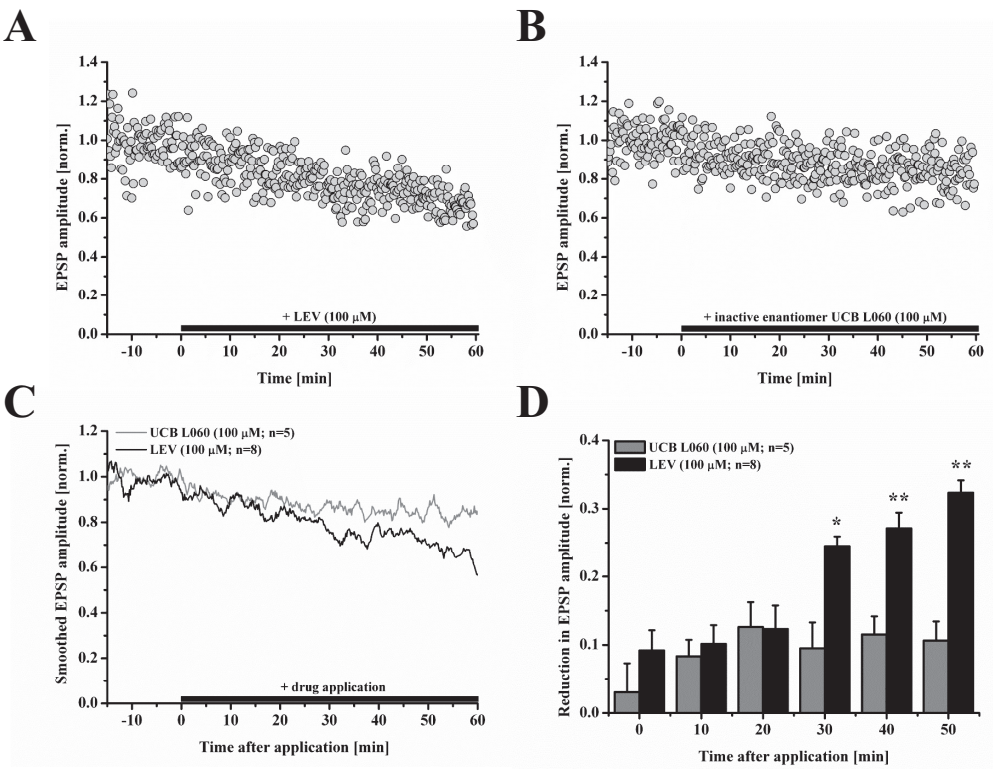

Fig. 1. LEV inhibits neurotransmission between synaptically coupled SCGNs. A and B, effects of LEV (100 μM) (A) and UCB L060 (100 μM) (B) on EPSP amplitudes at 0.1-Hz stimulation frequency. C, average EPSP amplitudes, determined by using a smoothed, eight-point, adjacent-average algorithm, for LEV and UCB l060. D, summary data on reductions in EPSP amplitudes. LEV caused significant reductions in EPSP amplitudes at ≥30 min. *, $P < 0.05$; **, $P < 0.01$, versus UCB L060.

(measured as I_{Ba}) in isolated SCGNs. Short-term bath application of LEV (100 μM, measured after 5 min) had no significant effect on whole-cell I_{Ba} amplitude, in comparison with control values (Supplemental Fig. 2). However, our results described above and the findings of some previous studies (Niespodziany et al., 2001; Yang et al., 2007; Yang and Rothman, 2009; Nowack et al., 2011) suggested that LEV actions might require extended application; therefore, we examined the effects of extracellular LEV pretreatment on whole-cell I_{Ba}. LEV pretreatment (100 μM, 1 h) significantly reduced Ca^{2+} current density and caused a corresponding decrease in maximal conductance, in comparison with both vehicle- and UCB L060 (100 μM)-pretreated control cells (Fig. 2; Table 1). Prolonged LEV pretreatment (100 μM, 3 h) reduced Ca^{2+} current density and conductance to a similar extent as that seen after 1-h LEV pretreatment (Fig. 2; Table 1), which demonstrates the saturability of LEV-induced Ca_V channel inhibition. LEV pretreatment (1 or 3 h) did not affect $V_{0.5}$, k, or V_{rev} (Fig. 2A; Table 1), which suggests that LEV does not alter the voltage dependence of activation. LEV pretreatment (100 μM, 1 h) significantly slowed Ca^{2+} current activation kinetics (Fig. 3A) but had no effect on steady-state inactivation (Fig. 3B). Whereas UCB L060 pretreatment (100 μM, 1 h) had no effect on current density or maximal Ca^{2+} channel conductance, small but statistically significant changes in $V_{0.5}$, k, and V_{rev}, compared with vehicle control values, were seen (Fig. 2; Table 1). UCB L060 pretreatment caused a slowing of activation kinetics similar to that seen with LEV under the same conditions (Fig. 3A) but was without effect on steady-state inactivation (Fig. 3B). Although these results indicate that UCB L060 interacts with Ca_V channels to affect aspects of activation gating, these interactions do not affect whole-cell I_{Ba} amplitude.

LEV Demonstrates Effects on Membrane Properties and AP Firing Behavior in SCGNs. The aforementioned results demonstrated that prolonged exposure to LEV inhibited Ca^{2+} influx through Ca_V channels. We next investigated the effects of LEV on intrinsic biophysical membrane properties and AP firing behavior in SCGNs. All experiments were performed after LEV pretreatment (1 h), to mirror the

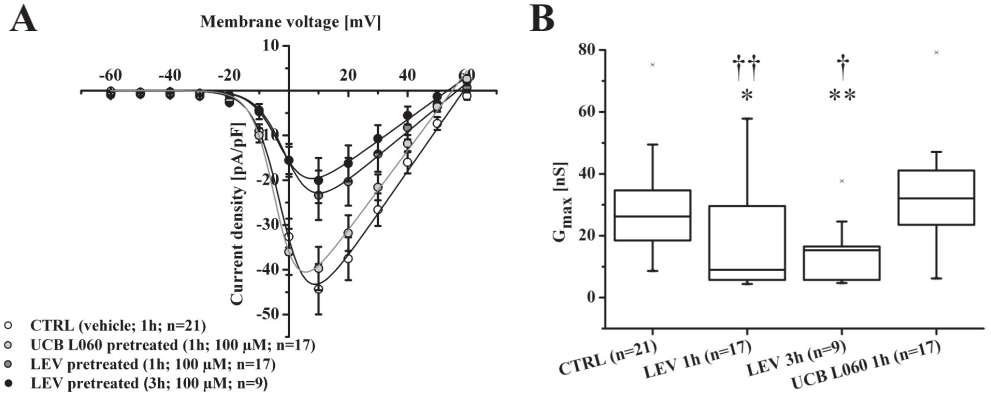

Fig. 2. Prolonged pretreatment with LEV reduces whole-cell Ca_V currents in SCGNs. The effects of LEV pretreatment (100 μM, 1 or 3 h) and UCB L060 pretreatment (100 μM, 1 h) on current density-voltage relationships (A) and maximal conductance (G_{max}) (B) were assessed. LEV pretreatment (1 h) caused significant decreases in both parameters; prolonged pretreatment (3 h) showed similar significant decreases, which suggests a saturating mechanism with slow onset. UCB L060 was without effect. †, $P < 0.05$; ††, $P < 0.01$, versus control (CTRL); *, $P < 0.05$; **, $P < 0.01$, versus UCB L060.

TABLE 1
Effects of LEV and UCB L060 (1-h pretreatment) on biophysical properties of whole-cell Ca^{2+} currents in SCGNs

	Vehicle (n = 21)	LEV		UCB L060 (n = 17)
		1 h (n = 17)	3 h (n = 9)	
Current density (measured at +10 mV), pA/pF	44.3 ± 5.6	23.4 ± 5.5**†	20.1 ± 5.1*†	39.7 ± 4.8
Maximal conductance, nS	30.6 ± 4.0	17.5 ± 4.1*††	15.3 ± 3.5**†	33.4 ± 4.7
Half-activation potential, mV	−2.2 ± 0.7	−4.3 ± 1.4	−3.6 ± 1.5	−5.2 ± 1.2*
Slope factor, mV	4.5 ± 0.2	4.1 ± 0.2	4.2 ± 0.7	3.7 ± 0.3*
Reversal potential, mV	58.0 ± 1.0	55.9 ± 1.3	54.1 ± 2.6	54.1 ± 1.2*

*$P < 0.05$ versus vehicle.
** $P < 0.01$ versus vehicle.
† $P < 0.05$ versus UCB L060 (Mann-Whitney U test).
†† $P < 0.01$ versus UCB L060 (Mann-Whitney U test).

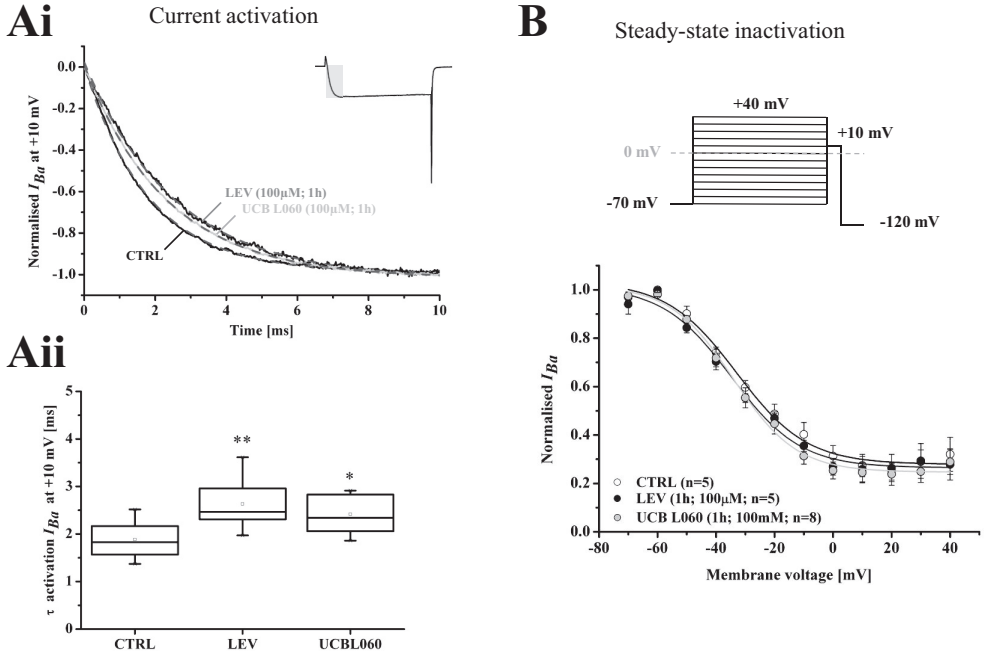

Fig. 3. LEV and UCB L060 treatments slow Ca_V current activation but do not modulate Ca_V channel steady-state inactivation. Sample traces illustrating Ca^{2+} current activation kinetics after 1-h pretreatment with vehicle (control), LEV (100 μM), or UCB L060 (100 μM) were recorded. A, i, exponential fits to the first 10 ms of the individual data sets to determine the time constant of activation (τ); inset, sample Ca^{2+} current trace (gray box, time window analyzed). ii, box plot of the time constants of current activation (at I_{max}). B, steady-state inactivation profiles with different pretreatments. *, $P < 0.05$; **, $P < 0.01$, versus control (CTRL).

conditions under which voltage-clamp experiments were performed. APs were evoked through depolarizing ramp current injection to trigger AP firing progressively in the recorded neuron, and the first AP of the evoked train was used for detailed analysis (Fig. 4; Table 2). To investigate the impact of reduced Ca^{2+} availability, the ECS Ca^{2+} concentration was substantially decreased in one of the experimental groups (low-Ca^{2+} ECS, with 0.2 mM Ca^{2+} and 1.8 mM Mg^{2+}). LEV pretreatment (1 h) caused a significant decrease in the amplitude of the AHP (the phase immediately after the repolarization phase of the triggered AP) under these conditions (Fig. 4, A and C; Table 2). The AHP has been reported to be reliant on activation of Ca^{2+}-dependent K^+ channels downstream from Ca^{2+} influx through $Ca_V2.2$ subunits in SCGNs (Davies et al., 1996; Martínez-Pinna et al., 2000) and, in support of a role for a Ca^{2+}-dependent conductance, incubation in low-Ca^{2+} ECS caused a significant decrease in AHP amplitude similar to that seen with LEV pretreatment (Fig. 4, A and C; Table 2). These results demonstrate a major effect of LEV on the AHP, consistent with a reduction in Ca^{2+} influx underlying this action. LEV pretreatment had no clear effect on resting membrane potential or on maximal AP amplitude or AP width (Fig. 4A; Table 2). With reduced extracellular Ca^{2+} levels, the AP width was significantly decreased ($P < 0.05$, control versus low-Ca^{2+} ECS) (Fig. 4A; Table 2). LEV prolonged AP latency, compared with both the control group and cells exposed to low-Ca^{2+} ECS (Fig. 4, A and B; Table 2). Other potential effects of LEV and low-Ca^{2+} ECS on cellular conductances involved in AP generation were analyzed in greater detail by using voltage PPPs (Fig. 5; Table 3). LEV or low-Ca^{2+} ECS had no effect on the depolarization rate (Fig. 5, A and C; Table 3). In contrast, LEV caused a significant slowing of repolarization, in comparison with the control and low-Ca^{2+} ECS groups (Fig. 5, B and D; Table 3). The effects on PPPs are consistent with additional, Ca^{2+}-independent, effects of LEV on membrane conductances, potentially involving voltage-dependent K^+ channels but not Na^+ channels, as discussed below.

Intracellular LEV Application Reduces Ca^{2+} Current Density and Conductance in SCGNs. The results presented above demonstrated that LEV exerted an inhibitory effect on whole-cell I_{Ba} amplitude that occurred with delayed onset, and they suggested that the ultimate site of action of LEV is not readily accessible after short-term external application. Such data may be consistent with an intracellular site of action for LEV. To test this hypothesis directly, we applied LEV intracellularly through inclusion in the patch pipette solution. In comparison with similarly applied UCB L060, intracellular LEV application significantly reduced Ca^{2+} current density (intracellular LEV: 20.0 ± 3.3

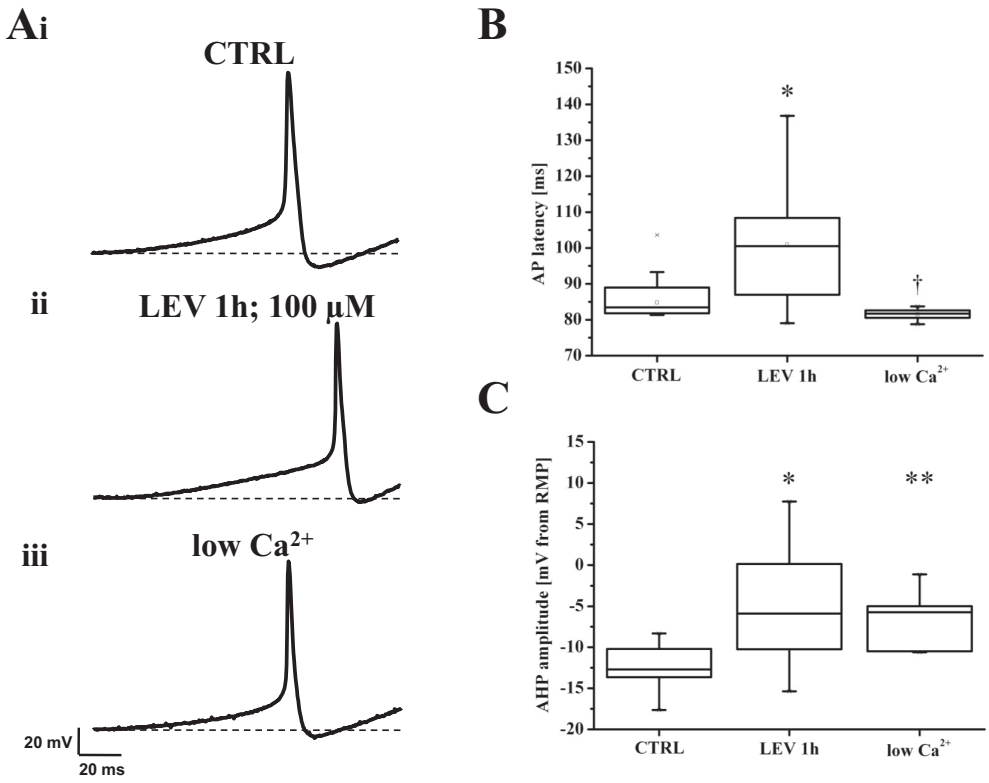

Fig. 4. LEV reduces the fast AHP in a Ca^{2+}-dependent manner and prolongs AP latency through a distinct pathway. A, representative voltage traces of the first evoked AP in response to ramp depolarization (0.5 pA/ms) with vehicle (control) (i), LEV (100 μM, 1 h) (ii), or low-Ca^{2+} ECS (iii). Dashed lines, respective resting membrane potentials. B and C, box plots summarizing prolongation of AP latency after LEV pretreatment (an effect independent of impaired Ca^{2+} availability) (B) and AHP reduction with LEV pretreatment or with low-Ca^{2+} ECS (C). *, $P < 0.05$; **, $P < 0.01$, versus control (CTRL); †, $P < 0.05$, versus 1-h LEV pretreatment.

TABLE 2
Effects of LEV pretreatment (100 μM, 1 h) and low-Ca^{2+} ECS on biophysical membrane properties and AP firing parameters in response to ramp depolarization in SCGNs

	Control (n = 9)	100 μM LEV, 1 h (n = 8)	Low-Ca^{2+} ECS (n = 6)
Resting membrane potential, mV	−53.6 ± 1.1	−56.4 ± 1.8	−56.0 ± 1.8
Maximal AP amplitude, mV	112.2 ± 2.4	113.1 ± 2.9	112.1 ± 4.0
AP width (at 0 mV), ms	3.1 ± 0.3	3.6 ± 0.3	2.7 ± 0.1*†
AP latency, ms	84.8 ± 3.8	100.9 ± 6.5*	81.5 ± 0.7†
AHP amplitude, mV	−12.5 ± 1.0	−5.0 ± 2.7*	−6.5 ± 1.5**

*$P < 0.05$ versus control.
** $P < 0.01$ versus control.
† $P < 0.05$ versus 1-h LEV pretreatment (unpaired Student's t test).

pA/pF, n = 16; intracellular UCB L060: 32.0 ± 3.2 pA/pF, n = 15; P = 0.019, Mann-Whitney U test) (Fig. 6A) and conductance (intracellular LEV: 14.6 ± 2.5 nS, n = 15; intracellular UCB L060: 26.0 ± 3.6 nS, n = 16; P = 0.022, Mann Whitney U test) (Fig. 6, B, C, and D). These measurements were made shortly (4–5 min) after establishment of the whole-cell patch-clamp configuration; this period allowed for complete cytoplasmic dialysis with the LEV-containing pipette solution and permits direct comparison with the results obtained after short-term extracellular LEV application (Supplemental Fig. 2). These data demonstrated a rapid onset of effect, which was not seen after external LEV application. Intracellular LEV application was as effective as LEV pretreatment (1 or 3 h) in reducing whole-cell Ca^{2+} conductance (Fig. 6C) and Ca^{2+} current density. In contrast, UCB L060 affected neither whole-cell Ca^{2+} conductance (Fig. 6D) nor Ca^{2+} current density, with pretreatment or intracellular application.

Finally, we tested whether direct injection of LEV or UCB L060 into the presynaptic partner in synaptically coupled SCGNs was able to affect synaptic transmission. Synaptic transmission was monitored as described above, and then either LEV or UCB L060 (1 mM in the pipette) was allowed to diffuse from a suction pipette into the presynaptic neurons for 2 to 3 min. Such intracellular application of LEV, but not UCB L060, significantly reduced EPSP amplitude at ≥20 min (Fig. 7). In this system, drug action at presynaptic terminals relies on drug diffusion from the somatic injection site, which renders the drug concentration inside the presynaptic cell body ~2.5% of the concentration in the pipette, as estimated on the basis of the color intensity of coinjected dye (Fast Green FCF) and corrected for the effect of molecular mass on diffusion (Mochida et al., 1996). With these caveats, these results confirm that LEV acts intracellularly at SCGN synapses, consistent with a mechanism whereby blockade of presynaptic Ca_V2 channels through an intracellular pathway leads to a reduction in synaptic transmission.

Discussion

LEV Inhibits Cholinergic Transmission. This study demonstrates that the prominent SV2A ligand LEV inhibits cholinergic transmission through actions on Ca_V channels in sympathetic neurons. We show that entry into the intracel-

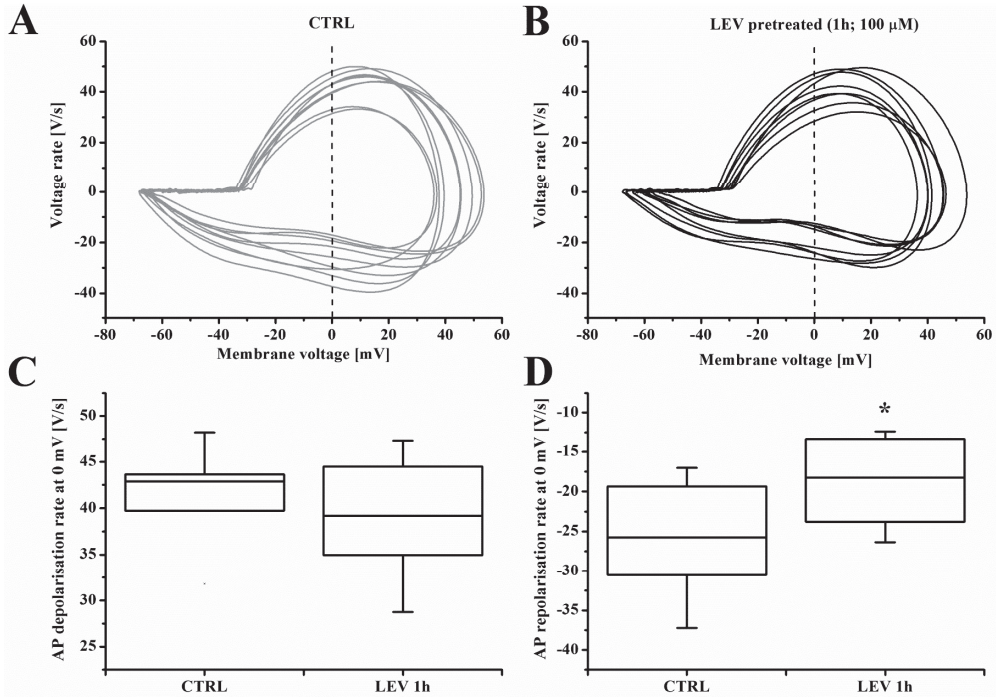

Fig. 5. LEV slows the AP repolarization phase but not the depolarization phase in voltage phase plane projections in SCGNs. A and B, phase plane projections from individual cells recorded with vehicle (control) (A) or LEV pretreatment (100 μM, 1 h) (B). C and D, box plots showing voltage rates measured at membrane voltages of 0 mV for depolarization (C) and repolarization (D) phases, revealing an inhibitory effect of LEV on the repolarization rate. *, $P < 0.05$, versus control (CTRL).

TABLE 3

Effects of LEV pretreatment (100 μM, 1 h) and low-Ca^{2+} ECS on depolarization and repolarization rates derived from voltage phase plane projections

Parameters were measured at 0 mV.

	Control (n = 9)	LEV, 1 h (n = 8)	Low-Ca^{2+} ECS (n = 6)
AP depolarization rate, V/s	41.0 ± 1.9	39.2 ± 2.2	44.2 ± 2.5
AP repolarization rate, V/s	−25.7 ± 2.4	−18.7 ± 2.0*	−28.2 ± 2.4†

*$P < 0.05$ versus control.
† $P < 0.05$ versus 1-h LEV pretreatment (unpaired Student's t test).

lular compartment before action at Ca_V channels is likely to be a rate-limiting step for LEV effects, as discussed below.

LEV Reduces Synaptic Transmission and Inhibits Ca_V Channels through an Intracellular Pathway. We demonstrate that LEV inhibits cholinergic transmission in SCGN synapses in a time-dependent manner, requiring 50 min to reach maximal inhibition. A requirement for prolonged LEV exposure (> 1 h) was reported for inhibition of evoked excitatory transmission in hippocampal CA1 neurons (Yang et al., 2007; Yang and Rothman, 2009; Meehan et al., 2011). In contrast, another study showed that LEV application (up to 6–10 h) had no effect on basal transmission but did reverse SV2A overexpression-mediated reductions in transmission (Nowack et al., 2011). A study with hippocampal dentate gyrus cells reported a rapid, readily reversible, LEV effect (Lee et al., 2009). We also demonstrate that LEV inhibits Ca_V channels, consistent with a major mechanism that limits AP-induced presynaptic Ca^{2+} entry and reduces cholinergic transmission between SCGNs. Although short-term LEV application was without effect, LEV pretreatment significantly reduced I_{Ba} amplitude. In this regard, $Ca_V2.2$ (N-type) subunits dominate somatic I_{Ba} in SCGNs and mediate acetylcholine release at SCGN synapses (Mochida et al., 1995, 2003; Bucci et al., 2011). LEV was reported to inhibit $Ca_V2.2$ and $Ca_V2.1$ (P/Q type) subunits (Surges et al., 2008). In general, such effects were measured in response to short-term LEV application and were reported to produce small irreversible reductions in Ca^{2+} current (Lukyanetz et al., 2002; Pisani et al., 2004; Costa et al., 2006; Martella et al., 2008); our data, which showed no short-term LEV effects, are in disagreement with those studies. However, Niespodziany et al. (2001) investigated the time dependence of LEV effects on Ca_V channels, and their finding that LEV required ≥30 min of perfusion to cause significant inhibition correlates well with our data. In the present study, LEV required prolonged external exposure to affect both Ca_V channels and cholinergic transmission. These findings are consistent with the hypothesis that accessing an intracellular site represents a rate-limiting step in LEV action. This hypothesis is fully supported by our major observation that intracellular application of LEV caused inhibition of Ca_V channels after 4 to 5 min of exposure; in marked contrast, short-term exposure to extracellular LEV for similar times was without effect. Intracellular LEV effects were similar in magnitude to those seen with prolonged (≥1-h) LEV pretreatment; together, these data are consistent with a common (intracellular) site of action. Furthermore, injection of LEV into the presynaptic partner in SCGN synapses was able to reduce transmitter release. No similar effects on synaptic transmission or Ca^{2+} influx were seen for the inactive LEV enantiomer UCB L060 with short-term or prolonged extracellular or intracellular application.

LEV inhibition of I_{Ba} amplitude after pretreatment occurred without changes in the voltage dependence of activa-

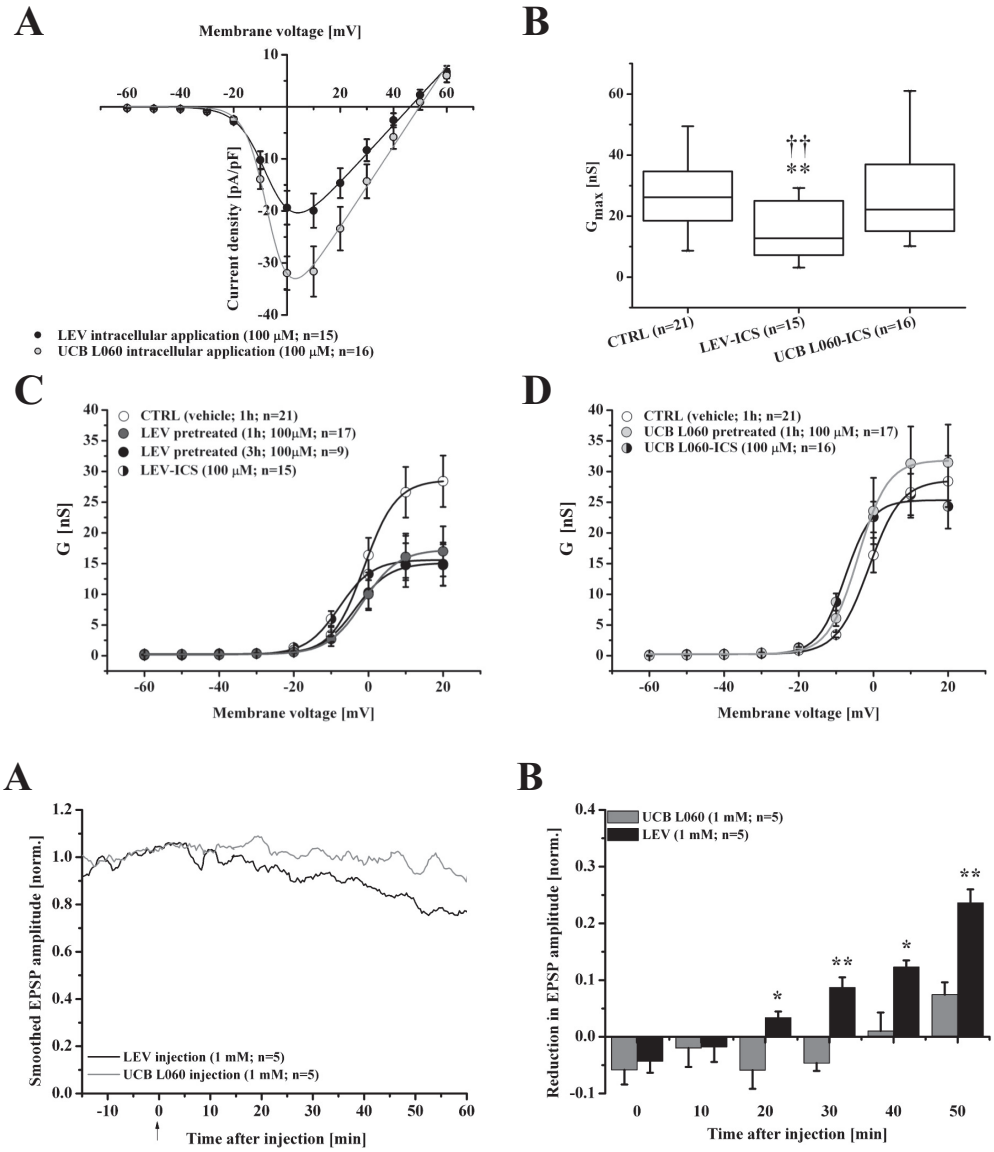

Fig. 6. Intracellular application of LEV through the patch electrode reduces whole-cell I_{Ba} in SCGNs. A and B, effects of intracellular application (4–5 min after establishment of the whole-cell patch-clamp configuration) of LEV (100 μM) and UCB L060 (100 μM) on Ca^{2+} current density (A) and maximal conductance (G_{max}) (B). C and D, summary of effects of different treatments with LEV (C) and UCB L060 (D) on conductance. LEV intracellular application and pretreatment (1 or 3 h) were equally effective in reducing conductance, and UCB L060 lacked effect regardless of treatment route. **, $P < 0.01$, versus control (CTRL); ††, $P < 0.01$, versus UCB L060. ICS, intracellular solution.

Fig. 7. Intracellular injection of LEV inhibits neurotransmission between synaptically coupled SCGNs. A, average EPSP amplitudes, determined by using a smoothed, eight-point, adjacent-average algorithm for effects of LEV (1 mM) and UCB L060 (1 mM) on EPSP amplitudes at 0.1-Hz stimulation frequency. B, summary data on reductions in EPSP amplitudes. LEV caused significant reductions in EPSP amplitudes at ≥20 min. *, $P < 0.05$; **, $P < 0.01$, versus UCB L060.

tion or steady-state inactivation; however, LEV did cause a slowing in I_{Ba} activation kinetics. UCB L060 also caused a slowing of activation kinetics. Moreover, UCB L060 pretreatment produced small but significant effects on the voltage dependence of activation properties. Together, these data suggest that UCB L060 can interact with Ca_V channels, but they also illustrate the importance of the molecule being in the correct conformation to cause the major effect of inhibition of Ca^{2+} influx.

LEV Affects Membrane Properties under Physiological Conditions. LEV effects on SCGN intrinsic membrane properties were consistent with reduced Ca^{2+} influx through Ca_V channels. LEV reduced the amplitude of the AHP, a phenomenon that is reliant on large and/or small Ca^{2+}-activated K^+ conductances and was reported to occur downstream from Ca^{2+} influx through $Ca_V2.2$ subunits in SCGNs (Davies et al., 1996; Martínez-Pinna et al., 2000). In support of this hypothesis, low-Ca^{2+} ECS reduced AHP amplitude to a similar extent as did LEV. Moreover, LEV caused a significant increase in AP latency, consistent with reduced neuronal excitability. The latter action was not reproduced in low-Ca^{2+} ECS, which suggests that LEV has additional, Ca^{2+}-independent effects. LEV was shown not to affect the AP depolarization rate, a process largely dependent on voltage-dependent Na^+ channel and potentially low-voltage-activated Ca^{2+} channel gating, which is consistent with reports of a lack of LEV effects on these conductances (Zona et al., 2001). In contrast, LEV did cause significant slowing of repolarization; this phenomenon was not reproduced by low-Ca^{2+} ECS and might be attributable to effects on voltage-dependent K^+ (K_V) channels. For example, LEV was reported to inhibit delayed rectifier K_V channels and to affect repetitive AP firing (Madeja et al., 2003), and such actions could contribute to the anticonvulsant profile of LEV. In this regard, it was of interest that LEV did not reproduce the reduction in AP width seen with low-Ca^{2+} ECS; the latter is consistent with previous reports on SCGNs that suggested a role for Ca^{2+} influx through Ca_V channels (Mochida and Kobayashi, 1986a,b). It may be speculated that LEV actions on K_V channels, inhibition of which typically broadens the AP, counteracted LEV-induced Ca_V channel effects on AP width. Although a major LEV effect on Ca_V channels is

reported here, actions on additional voltage-dependent ionic conductances may contribute to LEV effects on neuronal excitability and warrant separate investigations.

Other Factors May Be Involved in the LEV Mechanism of Action. We identify presynaptic Ca_V channels as a target for LEV, which acts through an intracellular pathway to inhibit Ca^{2+} influx and thus reduces transmitter release in SCGNs. LEV is a low-molecular weight ligand that is characterized by a polar surface area of 59.2 $Å^2$ and a measured logP value of −0.65 (unpublished observations), which suggests that the drug has relatively poor hydrophobic properties to cross cellular membranes readily. Prolonged exposure times, as used here, might allow LEV to enter cells through passive diffusion and to exert its effects on intracellular targets. More-detailed studies are required for full understanding of the kinetics of LEV permeability across cell membranes. Meehan et al. (2011) proposed that LEV action might be mediated through activity-dependent vesicular entry, with synaptic activity exposing intravesicular SV2A and allowing LEV to bind to and to enter the cell. In a similar manner, SV2 isoforms were proposed to bind botulinum A and E and tetanus neurotoxins and to facilitate their entry into neurons through synaptic vesicle endocytosis (Dong et al., 2006, 2008; Yeh et al., 2010). Once inside the cell, LEV may interact directly with Ca_V channels to cause inhibition, consistent with the rapid time course of inhibition after intracellular application. However, the lack of effect of UCB L060 (which is devoid of appreciable SV2A binding affinity) on Ca^{2+} influx and synaptic transmission may suggest that SV2A binding is a requirement for LEV effects on Ca_V channels. Related to this point, intracellular application might expose LEV to a larger pool of SV2A proteins and so accelerate effects on Ca_V channels. It is known that functionally defective SV2A can contribute to hyperexcitability disorders through excessive presynaptic Ca^{2+} accumulation and dysregulated transmitter release (Janz et al., 1999; Xu and Bajjalieh, 2001). SV2A-null mice develop a strong seizure phenotype (Crowder et al., 1999), and SV2A expression is decreased in human patients with epilepsy (van Vliet et al., 2009). Therefore, LEV binding to SV2A might stabilize defective Ca^{2+}-mediated release (Matveeva et al., 2008; Kaminski et al., 2009), and our data demonstrating that LEV acts to reduce presynaptic Ca^{2+} levels support such an effect. The functional effects of LEV on SV2A have not been fully established, although it was shown recently that LEV could reverse the disruptions in synaptic transmission caused by SV2A overexpression (Nowack et al., 2011). Experiments involving SV2A knockdown or knockout will be needed for complete determination of the role of SV2A in LEV action.

The finding that UCB L060 was without effect on I_{Ba} amplitude may support a stereospecific difference between LEV and UCB L060 effects on inhibition of Ca^{2+} influx through Ca_V channels. The high-affinity SV2A ligand brivaracetam does not bind or modulate Ca_V channels (Gillard et al., 2011) but is a Na^+ channel blocker, at least during short-term application (Zona et al., 2010). Such different effects suggest that SV2A binding per se may not dictate a common inhibitory mechanism; differences in molecular structures between SV2A ligands (and enantiomeric forms, at least for LEV) might confer differential ion channel inhibition as their ultimate mechanism of action.

In summary, our results strongly support a mechanism of action whereby LEV acts stereospecifically through an intracellular pathway to inhibit presynaptic Ca_V channels and to reduce transmitter release. Therefore, LEV is likely to possess a unique mechanism of action among AEDs. The novel involvement of SV2A in achieving these effects remains a focal point for further investigation (for example, by using different SV2A ligands and altering expression levels), to provide further insight into the therapeutic potential of LEV and its analogs.

Acknowledgments

We thank Shota Tanifuji (Tokyo Medical University) and Dimitris Xydas (University of Reading) for expert technical assistance. We thank the following UCB Pharma employees: Michaella Grossmann and Benedicte Danis for expert technical assistance; Karen Miller, Alain Matagne, and Isabelle Niespodziany for advice on the manuscript; and Doru Margineanu for productive initial discussions.

Authorship Contributions

Participated in research design: Vogl, Mochida, Wolff, Whalley, and Stephens.

Conducted experiments: Vogl and Mochida.

Contributed new reagents or analytic tools: Mochida, Wolff, Whalley, and Stephens.

Performed data analysis: Vogl and Mochida.

Wrote or contributed to the writing of the manuscript: Vogl, Mochida, Wolff, Whalley, and Stephens.

References

Bajjalieh SM, Frantz GD, Weimann JM, McConnell SK, and Scheller RH (1994) Differential expression of synaptic vesicle protein 2 (SV2) isoforms. *J Neurosci* **14:**5223–5235.

Bajjalieh SM, Peterson K, Shinghal R, and Scheller RH (1992) SV2, a brain synaptic vesicle protein homologous to bacterial transporters. *Science* **257:**1271–1273.

Bucci G, Mochida S, and Stephens GJ (2011) Inhibition of synaptic transmission and G protein modulation by synthetic $Ca_V2.2$ Ca^{2+} channel peptides. *J Physiol* **589:** 3085–3101.

Chang WP and Südhof TC (2009) SV2 renders primed synaptic vesicles competent for Ca^{2+}-induced exocytosis. *J Neurosci* **29:**883–897.

Costa C, Martella G, Picconi B, Prosperetti C, Pisani A, Di Filippo M, Pisani F, Bernardi G, and Calabresi P (2006) Multiple mechanisms underlying the neuroprotective effects of antiepileptic drugs against in vitro ischemia. *Stroke* **37:**1319–1326.

Crowder KM, Gunther JM, Jones TA, Hale BD, Zhang HZ, Peterson MR, Scheller RH, Chavkin C, and Bajjalieh SM (1999) Abnormal neurotransmission in mice lacking synaptic vesicle protein 2A (SV2A). *Proc Natl Acad Sci USA* **96:**15268–15273.

Custer KL, Austin NS, Sullivan JM, and Bajjalieh SM (2006) Synaptic vesicle protein 2 enhances release probability at quiescent synapses. *J Neurosci* **26:**1303–1313.

Davies PJ, Ireland DR, and McLachlan EM (1996) Sources of Ca^{2+} for different Ca^{2+}-activated K^+ conductances in neurones of the rat superior cervical ganglion. *J Physiol* **495:**353–366.

De Smedt T, Raedt R, Vonck K, and Boon P (2007a) Levetiracetam: part II, the clinical profile of a novel anticonvulsant drug. *CNS Drug Rev* **13:**57–78.

De Smedt T, Raedt R, Vonck K, and Boon P (2007b) Levetiracetam: the profile of a novel anticonvulsant drug–part I: preclinical data. *CNS Drug Rev* **13:**43–56.

Dong M, Liu H, Tepp WH, Johnson EA, Janz R, and Chapman ER (2008) Glycosylated SV2A and SV2B mediate the entry of botulinum neurotoxin E into neurons. *Mol Biol Cell* **19:**5226–5237.

Dong M, Yeh F, Tepp WH, Dean C, Johnson EA, Janz R, and Chapman ER (2006) SV2 is the protein receptor for botulinum neurotoxin A. *Science* **312:**592–596.

Feany MB, Lee S, Edwards RH, and Buckley KM (1992) The synaptic vesicle protein SV2 is a novel type of transmembrane transporter. *Cell* **70:**861–867.

Gillard M, Chatelain P, and Fuks B (2006) Binding characteristics of levetiracetam to synaptic vesicle protein 2A (SV2A) in human brain and in CHO cells expressing the human recombinant protein. *Eur J Pharmacol* **536:**102–108.

Gillard M, Fuks B, Leclercq K, and Matagne A (2011) Binding characteristics of brivaracetam, a selective, high affinity SV2A ligand in rat, mouse and human brain: relationship to anti-convulsant properties. *Eur J Pharmacol* **664:**36–44.

Gillard M, Fuks B, Michel P, Vertongen P, Massingham R, and Chatelain P (2003) Binding characteristics of [^{3}H]UCB 30889 to levetiracetam binding sites in rat brain. *Eur J Pharmacol* **478:**1–9.

Grünewald R (2005) Levetiracetam in the treatment of idiopathic generalized epilepsies. *Epilepsia* **46 (Suppl 9):**154–160.

Janz R, Goda Y, Geppert M, Missler M, and Südhof TC (1999) SV2A and SV2B function as redundant Ca^{2+} regulators in neurotransmitter release. *Neuron* **24:** 1003–1016.

Kaminski RM, Gillard M, Leclercq K, Hanon E, Lorent G, Dassesse D, Matagne A, and Klitgaard H (2009) Proepileptic phenotype of SV2A-deficient mice is associated with reduced anticonvulsant efficacy of levetiracetam. *Epilepsia* **50:**1729–1740.

Kenda BM, Matagne AC, Talaga PE, Pasau PM, Differding E, Lallemand BI, Frycia AM, Moureau FG, Klitgaard HV, Gillard MR, et al. (2004) Discovery of 4-substituted pyrrolidone butanamides as new agents with significant antiepileptic activity. *J Med Chem* **47:**530–549.

Klitgaard H, Matagne A, Gobert J, and Wülfert E (1998) Evidence for a unique profile of levetiracetam in rodent models of seizures and epilepsy. *Eur J Pharmacol* **353:**191–206.

Lee CY, Chen CC, and Liou HH (2009) Levetiracetam inhibits glutamate transmission through presynaptic P/Q-type calcium channels on the granule cells of the dentate gyrus. *Br J Pharmacol* **158:**1753–1762.

Lukyanetz EA, Shkryl VM, and Kostyuk PG (2002) Selective blockade of N-type calcium channels by levetiracetam. *Epilepsia* **43:**9–18.

Lynch BA, Lambeng N, Nocka K, Kensel-Hammes P, Bajjalieh SM, Matagne A, and Fuks B (2004) The synaptic vesicle protein SV2A is the binding site for the antiepileptic drug levetiracetam. *Proc Natl Acad Sci USA* **101:**9861–9866.

Madeja M, Margineanu DG, Gorji A, Siep E, Boerrigter P, Klitgaard H, and Speckmann EJ (2003) Reduction of voltage-operated potassium currents by levetiracetam: a novel antiepileptic mechanism of action? *Neuropharmacology* **45:**661–671.

Martella G, Bonsi P, Sciamanna G, Platania P, Madeo G, Tassone A, Cuomo D, and Pisani A (2009) Seletracetam (UCB 44212) inhibits high-voltage-activated Ca^{2+} currents and intracellular Ca^{2+} increase in rat cortical neurons in vitro. *Epilepsia* **50:**702–710.

Martella G, Costa C, Pisani A, Cupini LM, Bernardi G, and Calabresi P (2008) Antiepileptic drugs on calcium currents recorded from cortical and PAG neurons: therapeutic implications for migraine. *Cephalalgia* **28:**1315–1326.

Martínez-Pinna J, Davies PJ, and McLachlan EM (2000) Diversity of channels involved in Ca^{2+} activation of K^+ channels during the prolonged AHP in guinea-pig sympathetic neurons. *J Neurophysiol* **84:**1346–1354.

Matagne A, Margineanu DG, Kenda B, Michel P, and Klitgaard H (2008) Anticonvulsive and anti-epileptic properties of brivaracetam (UCB 34714), a high-affinity ligand for the synaptic vesicle protein, SV2A. *Br J Pharmacol* **154:**1662–1671.

Matveeva EA, Vanaman TC, Whiteheart SW, and Slevin JT (2008) Levetiracetam prevents kindling-induced asymmetric accumulation of hippocampal 7S SNARE complexes. *Epilepsia* **49:**1749–1758.

Meehan AL, Yang X, McAdams BD, Yuan L, and Rothman SM (2011) A new mechanism for antiepileptic drug action: vesicular entry may mediate the effects of levetiracetam. *J Neurophysiol* **106:**1227–1239.

Mochida S and Kobayashi H (1986a) Activation of M2 muscarinic receptors causes an alteration of action potentials by modulation of Ca entry in isolated sympathetic neurons of rabbit. *Neurosci Lett* **72:**199–204.

Mochida S and Kobayashi H (1986b) Effects of Ca antagonists on the action potential and their relationship to the muscarinic ACh actions in isolated sympathetic neurons of rabbit. *Neurosci Lett* **72:**205–210.

Mochida S, Saisu H, Kobayashi H, and Abe T (1995) Impairment of syntaxin by botulinum neurotoxin C1 or antibodies inhibits acetylcholine release but not Ca^{2+} channel activity. *Neuroscience* **65:**905–915.

Mochida S, Sheng ZH, Baker C, Kobayashi H, and Catterall WA (1996) Inhibition of neurotransmission by peptides containing the synaptic protein interaction site of N-type Ca^{2+} channels. *Neuron* **17:**781–788.

Mochida S, Westenbroek RE, Yokoyama CT, Itoh K, and Catterall WA (2003) Subtype-selective reconstitution of synaptic transmission in sympathetic ganglion neurons by expression of exogenous calcium channels. *Proc Natl Acad Sci USA* **100:**2813–2818.

Niespodziany I, Klitgaard H, and Margineanu DG (2001) Levetiracetam inhibits the high-voltage-activated Ca^{2+} current in pyramidal neurones of rat hippocampal slices. *Neurosci Lett* **306:**5–8.

Nowack A, Malarkey EB, Yao J, Bleckert A, Hill J, and Bajjalieh SM (2011) Levetiracetam reverses synaptic deficits produced by overexpression of SV2A. *PLoS One* **6:**e29560.

Patsalos PN (2000) Pharmacokinetic profile of levetiracetam: toward ideal characteristics. *Pharmacol Ther* **85:**77–85.

Pisani A, Bonsi P, Martella G, De Persis C, Costa C, Pisani F, Bernardi G, and Calabresi P (2004) Intracellular calcium increase in epileptiform activity: modulation by levetiracetam and lamotrigine. *Epilepsia* **45:**719–728.

Schiemann-Delgado J, Yang H, Loge Cde L, Stalvey TJ, Jones J, Legoff D, and Mintz M (2012) A long-term open-label extension study assessing cognition and behavior, tolerability, safety, and efficacy of adjunctive levetiracetam in children aged 4 to 16 years with partial-onset seizures. *J Child Neurol* **27:**80–89.

Stephens GJ and Mochida S (2005) G protein $\beta\gamma$ subunits mediate presynaptic inhibition of transmitter release from rat superior cervical ganglion neurones in culture. *J Physiol* **563:**765–776.

Stephens GJ, Page KM, Bogdanov Y, and Dolphin AC (2000) The α1B Ca^{2+} channel amino terminus contributes determinants for β subunit-mediated voltage-dependent inactivation properties. *J Physiol* **525:**377–390.

Surges R, Volynski KE, and Walker MC (2008) Is levetiracetam different from other antiepileptic drugs? Levetiracetam and its cellular mechanism of action in epilepsy revisited. *Ther Adv Neurol Disord* **1:**13–24.

van Vliet EA, Aronica E, Redeker S, Boer K, and Gorter JA (2009) Decreased expression of synaptic vesicle protein 2A, the binding site for levetiracetam, during epileptogenesis and chronic epilepsy. *Epilepsia* **50:**422–433.

Xu T and Bajjalieh SM (2001) SV2 modulates the size of the readily releasable pool of secretory vesicles. *Nat Cell Biol* **3:**691–698.

Yang XF and Rothman SM (2009) Levetiracetam has a time- and stimulation-dependent effect on synaptic transmission. *Seizure* **18:**615–619.

Yang XF, Weisenfeld A, and Rothman SM (2007) Prolonged exposure to levetiracetam reveals a presynaptic effect on neurotransmission. *Epilepsia* **48:**1861–1869.

Yeh FL, Dong M, Yao J, Tepp WH, Lin G, Johnson EA, and Chapman ER (2010) SV2 mediates entry of tetanus neurotoxin into central neurons. *PLoS Pathog* **6:**e1001207.

Zona C, Niespodziany I, Marchetti C, Klitgaard H, Bernardi G, and Margineanu DG (2001) Levetiracetam does not modulate neuronal voltage-gated Na^+ and T-type Ca^{2+} currents. *Seizure* **10:**279–286.

Zona C, Pieri M, Carunchio I, Curcio L, Klitgaard H, and Margineanu DG (2010) Brivaracetam (UCB 34714) inhibits Na^+ current in rat cortical neurons in culture. *Epilepsy Res* **88:**46–54.

Address correspondence to: Dr. Gary Stephens, School of Pharmacy, University of Reading, Whiteknights, P.O. Box 228, Reading RG6 6AJ, UK. E-mail: g.j.stephens@reading.ac.uk